Delft University of Technology

Subwavelength spinning of particles in vector cosine-Gaussian field with radial polarization

Zhao, Rui; Jiang, Min; Zhang, Shuoshuo; Man, Zhongsheng; Wang, Benyi; Ge, Xiaolu; Zhang, Wenfei; Zhang, Yuquan; Fu, Shenggui

Important note
To cite this publication, please use the final published version (if applicable).
Please check the document version above.

Subwavelength spinning of particles in vector cosine-Gaussian field with radial polarization

Rui Zhao [a], Min Jiang [b], Shuoshuo Zhang [c], Zhongsheng Man [a,d,*], Benyi Wang [a], Xiaolu Ge [a], Wenfei Zhang [a], Yuquan Zhang [c], Shenggui Fu [a]

[a] *School of Physics and Optoelectronic Engineering, Shandong University of Technology, Zibo 255000, China*
[b] *Optics Research Group, Delft University of Technology, Department of Imaging Physics, Lorentzweg 1, 2628CJ Delft, The Netherlands*
[c] *Nanophotonics Research Center, Shenzhen Key Laboratory of Micro-Scale Optical Information Technology & Institute of Microscale Optoelectronics, Shenzhen University, Shenzhen 518060, China*
[d] *Collaborative Innovation Center of Light Manipulations and Application, Shandong Normal University, Jinan 250358, China*

A B S T R A C T

A new type of radially polarized (RP) cosine-Gaussian (CG) field is proposed. Through the analytical model, it is found that such RP CG beam exhibits completely different focusing properties from the reported RP plane waves. More importantly, a stable three-dimensional trap of Rayleigh particle accompanied by a subwavelength spin motion can be easily achieved using this RP CG beam.

1. Introduction

Since the first practical laser traps of micrometer sized particles demonstrated by Ashkin in 1970 [1], optical tweezer has become powerful tools to capture and manipulate various objects, arising from its unique noncontact and noninvasive advantages [2–19]. Recently, light-induced rotation [20–25] attracts great attentions due to some practical and useful applications ranging from micro-rotors [26] to optical spanners [27], as well as cell orientation [28] and photonic devices [10]. Physically, two dynamic properties of light in terms of linear momentum (LM) and angular momentum (AM) play crucial roles in the light-matter interactions of trapping [29–32]. There are two categories of LMs including spin linear momentum (SLM) and orbital linear momentum (OLM). SLM is proportional to the curl of the spin density of the light, whereas the OLM is proportional to the radiation force on a particle [33,34]. Similarly, the AM of light can also be separated into two parts: spin angular momentum (SAM) and orbital angular momentum (OAM). Being related to the vectorial nature of light, SAM is intrinsic, resulting in the rotation of a particle around its axis [35]. In contrast, the OAM of light is associated with the azimuthal dependence of the optical phase, inducing the rotation of particle around the optical axis [36].

In addition, the state of polarization (SoP) of light is of primary importance in modern physics. Apart from scalar fields with spatially homogeneous SoP, such as linear, elliptical, and circular polarizations, a light beam admits spatially-variant SoP, i.e. vector field [37–54]. As a kind of typical vector fields, radially polarized (RP) beam, which

have all the SoPs in the beam cross section to be linearly polarized and arranged along the radial direction, has attracted significant interest due to the unique features compared with homogeneously polarized beams. Usually, it is believed that a RP beam can create a strong on-axis longitudinal and non-propagating electric field when focusing by a high numerical (NA) [55–58] objective lens, which makes the RP beam better for many applications.

In this Letter, we propose a new type of cosine-Gaussian (CG) beam with radial polarization. Applying the Richards and Wolf vectorial diffraction methods, the explicit expressions are presented to calculate the strength vectors and energy flux of the three-dimensional electric and magnetic fields. By calculations, the intensity structure of the tightly focused RP CG beam is found to exhibit strong on-axis transverse electric field, whereas the longitudinal electric field bears a shape similar to a dipole, having two lobes located symmetrically with respect to the y axis. The magnetic field is totally transversely polarized in the focal region, which has nearly the same pattern as that of the transverse electric field. In additional, the optical force and torque on a Rayleigh particle produced by the focused RP CG beam is also studied in detail, which indicates a stable three-dimensional trap can be achieved. Meanwhile, the trapped particles always have a spin motion.

2. Radially polarized cosine-Gaussian beam and its tight focusing property

Generally, light from a laser without specially designed cavity is linearly polarized Gaussian beam, and its electric field expression can
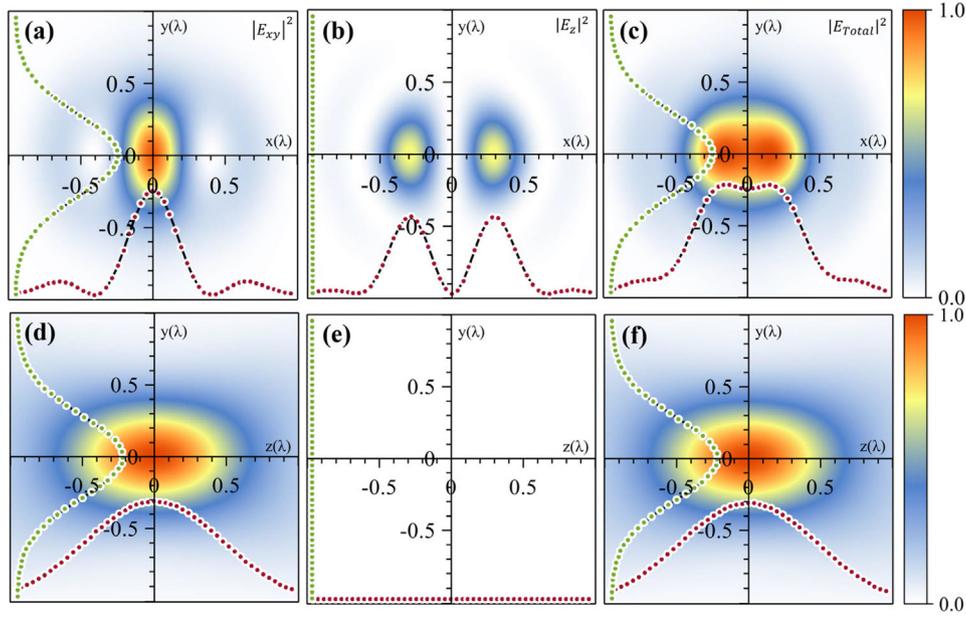

Fig. 1. Normalized electric field intensity distributions in the focal (top raw) and the through-focus planes (bottom row) of the focused RP CG beam when $\phi_0 = 0$. The columns from left to right correspond to the transverse component, longitudinal component, and their total. The insets in each image show the intensity profiles along axes, respectively.

be written mathematically as

$$\mathbf{E}_1(r, \phi, z) = A \exp\left(-\frac{r^2}{\omega_0^2}\right)\left(\cos\phi_0\hat{\mathbf{e}}_x + \sin\phi_0\hat{\mathbf{e}}_y\right), \tag{1}$$

where A is the radial profile of the field; r and ϕ denote the polar radius and the azimuthal angle, respectively; ω_0 is the radius of the beam waist; ϕ_0 is the initial phase determining the polarization direction in the beam cross section; $\hat{\mathbf{e}}_x$ and $\hat{\mathbf{e}}_y$ denote unit vectors directed along x and y axes, respectively, of the linear polarization. Eq. (1) can also be expressed with respect to the radial and azimuthal polarization basis $\{\hat{\mathbf{e}}_r, \hat{\mathbf{e}}_a\}$ through the relations $\hat{\mathbf{e}}_x = \cos\phi\hat{\mathbf{e}}_r - \sin\phi\hat{\mathbf{e}}_a$ and $\hat{\mathbf{e}}_y = \sin\phi\hat{\mathbf{e}}_r + \cos\phi\hat{\mathbf{e}}_a$ as

$$\mathbf{E}_1(r, \phi, z) = A\exp\left(-\frac{r^2}{\omega_0^2}\right)\left[\cos\left(\phi - \phi_0\right)\hat{\mathbf{e}}_r - \sin\left(\phi - \phi_0\right)\hat{\mathbf{e}}_a\right]. \tag{2}$$

When the linearly polarized Gaussian beam passes through a radial-type extractor [59], the azimuthal polarization component will be filtered out, then a new type of CG beam can be obtained:

$$\mathbf{E}_2(r, \phi, z) = A\exp\left(-\frac{r^2}{\omega_0^2}\right)\cos\left(\phi - \phi_0\right)\hat{\mathbf{e}}_r. \tag{3}$$

Tight focusing is highly desirable, ranging from microimaging to optical tweezers, as well as high density storage. In such a system, a high NA objective lens is introduced, and the electromagnetic field in the image space should be analyzed with Richards and Wolf vectorial diffraction theory [60], because the contribution of the input polarization cannot be neglected. When the incident beam is described by Eq. (3), the electric and magnetic fields at an arbitrary observation point $P(\rho, \varphi, z)$ in the focal volume of a high NA objective lens can be obtained as [60–64]

$$\begin{bmatrix} \mathbf{E} \\ \mathbf{H} \end{bmatrix} = -\frac{ikf}{2\pi}\int_0^\alpha\int_0^{2\pi}\sqrt{\cos\theta}e^{\{ik[-\rho\sin\theta\cos(\phi-\varphi)+z\cos\theta]\}}$$
$$\times Ae^{\left(-\frac{\beta^2\sin^2\theta}{\sin^2\alpha}\right)}\cos\left(\phi - \phi_0\right)\begin{bmatrix} \mathbf{V}_E \\ \mathbf{V}_H \end{bmatrix}\sin\theta d\phi d\theta, \tag{4}$$

where k is the wave number in the image space, f is the focal distance, $\alpha = \arcsin(NA/n)$ is the semi-aperture on the image side, where NA is the numerical aperture of the focusing objective lens and n is the refractive index in the image space, and β is the ratio of the pupil radius to the beam waist. θ and ϕ depict the tangential angle with respect to

the z axis and azimuthal angle with respect to the x axis in the object space, respectively. The vectors VE and VH represent the electric and magnetic field polarization vectors in the image space with the three mutually perpendicular components being

$$\begin{bmatrix} \mathbf{V}_E \\ \mathbf{V}_H \end{bmatrix} = \begin{bmatrix} \cos\theta\cos\phi\hat{\mathbf{e}}_x + \cos\theta\sin\phi\hat{\mathbf{e}}_y + \sin\theta\hat{\mathbf{e}}_z \\ -B\sin\phi\hat{\mathbf{e}}_x + B\cos\phi\hat{\mathbf{e}}_y \end{bmatrix}, \tag{5}$$

Here, $B = \sqrt{\varepsilon/\mu}$, where ε and μ are, respectively, the electric permittivity and magnetic permeability. In terms of the 3D electric and magnetic fields expressed by Eq. (5), the energy current is obtained from a determination of the time-averaged Poynting vector [60,65–67]

$$\mathbf{S} \propto \text{Re}\left(\mathbf{E}\times\mathbf{H}^*\right), \tag{6}$$

where the asterisk denotes complex conjugation. We can then study the tight focusing properties of the new type of RP CG beam based on Eqs. (4)–(6). All length measurements are in unit of wavelength, therefore, $\lambda = 1$; $\beta = 1$, NA $= 1.26$, and $n = 1.33$ are used in the following calculations.

Now we calculate the electric field distributions in the focal region under the above focusing conditions. Fig. 1 shows the transverse, longitudinal, and total field intensity distributions in the focal and through-focus planes of the proposed RP CGB when $\phi_0 = 0$. Apparently, the circular symmetry for the total field of the focused RP CGB is broken, which is a hot spot and exhibits on-axis elliptically symmetric intensity distributions [Figs. 1(c) and 1(f)]. Furthermore, the on-axis field is primarily contributed by the transverse component [Figs. 1(a) and 1(d)], whereas the outer part of the field is contributed by the longitudinal component [Fig. 1(b)]. Additionally, compared with the longitudinal component, the transverse component is much stronger and dominates the total field. These peculiar properties are much different from the focusing characteristics of previously reported RP beams in the literatures [55,57], which provides new insights into the fundamental properties of RP beams and may lead to new applications

The corresponding magnetic field intensity distributions in the focal and through-focus planes are also calculated, as depicted in Fig. 2. Unlike the electric field distribution [Fig. 1], the magnetic field of the focused RP CG beam with $\phi_0 = 0$ is all contributed by the transverse component. Meanwhile, we can see that the magnetic field has nearly the same pattern compared with the transverse component of the electric field [Figs. 1(a) and 1(d)].
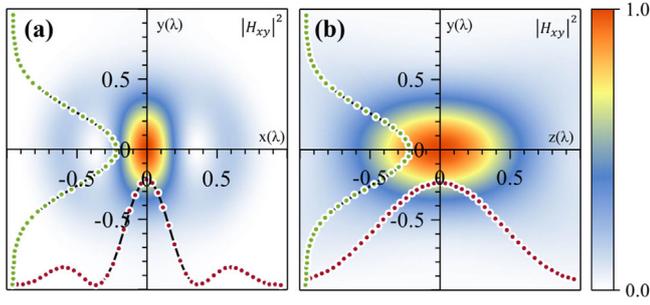
Fig. 2. Normalized magnetic field intensity distributions (a) in the focal and (b) through-focus planes of the focused RP CG beam when $\Box\phi_0 = 0$. The insets in each image show the intensity profiles along axes, respectively.
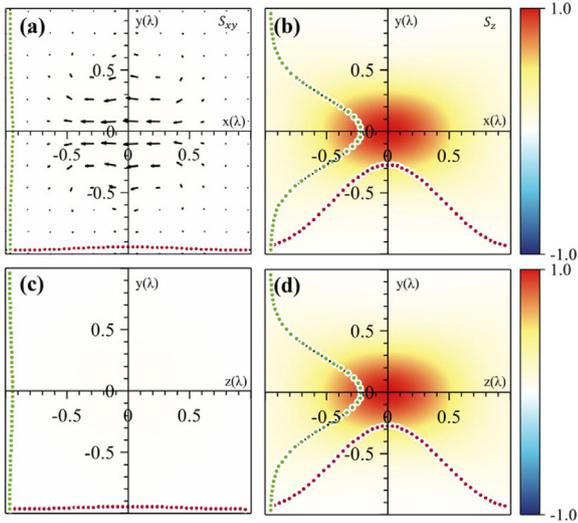

Fig. 3. Calculated transverse (left column) and longitudinal (right column) Poynting vectors distributions of the focused RP CG when $\Box\phi_0 = 0$ in the focal (top row) and through-focus (bottom row) planes. Black arrows indicate the direction of the transverse energy flow. The insets in each image show the energy flow profiles along axes, respectively.

Fig. 3 shows the normalized transverse and longitudinal Poynting vector distributions in the focal and through-focus planes for the beam shown in Figs. 1 and 2. Usually, no transverse energy flows near focus can be found for the input RP plane waves [65–68]. However, we can see from Figs. 3(a) and 3(c) that weak transverse energy flows [with values very close to zero, which can be seen from the energy flow profiles along axes] appear here, which always flow in the negative direction of the x-axis. Compared with the transverse component of the Poynting vector, the longitudinal energy flow is much stronger and exhibits nearly the same patterns in the x–y and y–z planes shown in Figs. 3(b) and 3(d).

3. Optical force and torque on Rayleigh particles

In this section, we study the generation of force and torque when light interacts with particles. We consider the case of particles much smaller than the trapping wavelength where one can make use of Rayleigh approximation. And the optical response of a nanostructure can be modeled as that of a dipole or a collection of dipoles. The dipolar polarizability determines the strength of interaction with an optical field. For a Rayleigh spherical particle of radius a and permittivity ε_1 placed in the above focused field propagating in a medium with permittivity ε and permeability μ, this can be written as [69]

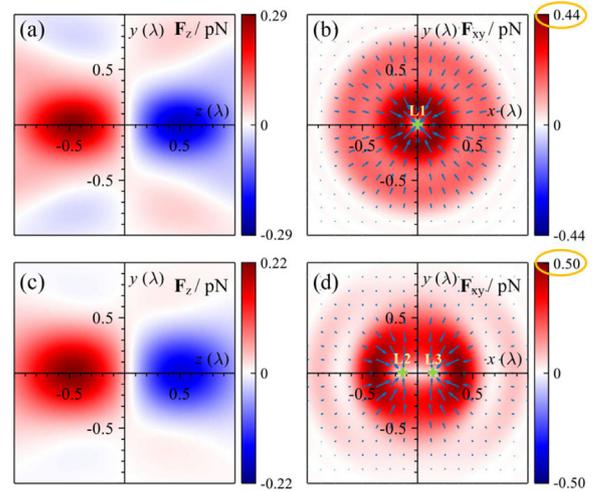$$\alpha = \frac{\alpha_0}{1 - i(2/3)k^3 a_0},\tag{7}$$

Fig. 4. Longitudinal and transverse forces on distributions on the Rayleigh particle with $n_1 = 1.59 + 0.005i$ generated by the tightly focused normal RP (top row) and RP CG (bottom row) beams in the y–z ($x = 0$) and x–y ($z = 0.06\lambda$) planes, respectively. The arrows represent the direction of the force. Point L1, L2, and L3 represent equilibrium positions.

where α_0 is the point-like particle polarizability given by [70]

$$\alpha_0 = 4\pi\varepsilon a^3 \frac{\varepsilon_1/\varepsilon - 1}{\varepsilon_1/\varepsilon + 2},\tag{8}$$

Based on the momentum conservation, transferring LM from light beam to particle generates an optical force, which can be written as the sum of three terms [71]

$$\langle \mathbf{F} \rangle = \frac{1}{4}\text{Re}\left\{\alpha\right\}\nabla\left|\mathbf{E}\right|^2 + \frac{1}{2}\text{Im}\left\{\alpha\right\}k\sqrt{\frac{\mu}{\varepsilon}}\text{Re}\left(\mathbf{E}\times\mathbf{H}^*\right)$$
$$+ \frac{1}{2}\text{Im}\left\{\alpha\right\}\text{Re}\left[i\left(\mathbf{E}\cdot\nabla\right)\mathbf{E}^*\right],\tag{9}$$

The first term in Eq. (9) denotes the force arising from the gradient of the electric intensity, which permits three-dimensional confinement in optical tweezers and dominates the total optical forces. The second term, responsible for the radiation pressure, correspond to a force in the propagation direction. The third term is the curl force associated with the non-uniform distribution of the spin angular momentum.

We now examine the mechanical consequences when the focused field interacts with particles. Consider a Rayleigh particle with radius $a = 30$ nm and complex refractive index $n_1 = 1.59 + 0.005i$. The real part of the complex refractive index n_1 is chosen based on the value of polystyrene particles, which are often used as samples in optical tweezers. Here, we assign a small imaginary part to the refractive index n_1 to characterize the absorption of light by the particle. To examine the three-dimensional trapping capability of the focused RP CG beam, we first calculate the longitudinal force distributions in the y–z plane when $x = 0$, depicted in Fig. 4(a). For the sake of comparison, the corresponding distributions of a normal RP input beam is also calculated under the same focusing conditions, shown in Fig. 4(c). The positive and negative longitudinal forces indicate that they are directed along the $+z$ and $-z$ axes, respectively. By calculations, the equilibrium position where $F_z = 0$ is found at about $z = 0.06\lambda$. On the two sides of the equilibrium position, the directions of the longitudinal forces are opposite, and they both point to the equilibrium position. As a result, a stable longitudinal trap for the Rayleigh particle is possible for both normal RP and RP CG input beams. Figs. 4(b) and 4(d) show the transverse force distributions in the x–y plane when $z = 0.06\lambda$ for the above two input beams, where the arrow denotes the direction of the transverse force. From the arrows in Fig. 4(b) we can see the transverse force directs one position located on axis to produce a force balance, which means particle can be trapped there. On the contrary,
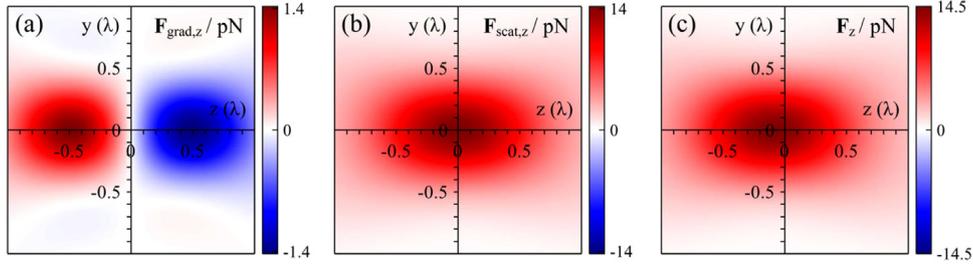
Fig. 5. (a) Gradient force, (b) scattering force, and (c) total force on a gold nanoparticle with $n_1 = 0.48646 + 2.2354i$ in the y–z ($x = 0$) plane, produced by the tightly focused RP CG beam.
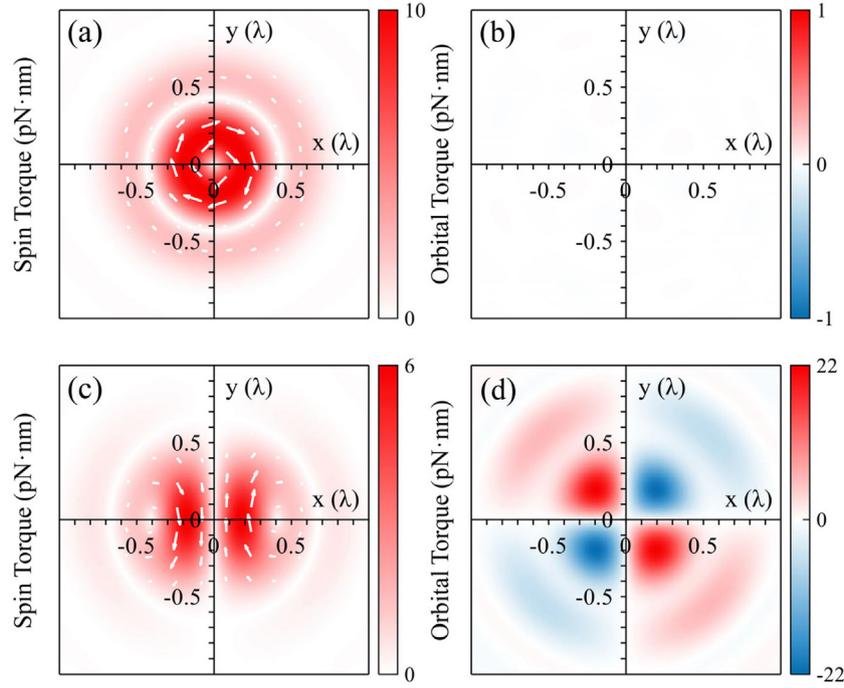

Fig. 6. The transverse spin torque and longitudinal orbital torque distributions on the Rayleigh particle with $n_1 = 1.59 + 0.005i$ generated by the focused normal RP (top row) and RP CG (bottom row) beams in the x–y ($z = 0.06\lambda$) plane. The arrow represents the direction of the torque.

double equilibrium positions located symmetrically with respect to the y axis appears for the RP CG input beam. The shift of equilibrium position from optical axis to outside of it is very important, since it may bring some new effects in light matter interactions. In addition, the transverse force is found to be stronger than that of normal RP beam. The maximum transverse force is about 1.16 times bigger than that of normal RP input field, which can be seen in Figs. 4(b) and 4(d). So the RP CG input beam can be expected to produce a more stable transverse trapping.

The magnitude of the optical force is closely correlated to the optical properties of particles. Different from dielectric particles, metallic particles, such as gold particles, are generally considered difficult to trap with conventional optical tweezers due to the strong absorption and scattering of light. Fig. 5 shows the longitudinal optical force on a gold nanoparticle with $n_1 = 0.48646 + 2.2354i$, produced by a tightly focused radially-polarized Cosine-Gaussian beam. Since the scattering force [Fig. 5(b)] is one order of magnitude larger than the gradient force [Fig. 5(a)], the total force is always positive for arbitrary positions in the y–z plane, as depicted in Fig. 5(c). Therefore, the gold nanoparticle will be pushed away from the focus, manifesting a non-trapped phenomenon of metallic particle for the proposed RP CG beam.

The transfer of the LM from light to the particle induces an optical force, whereas the transfer of the AM leads to optical torques. For

the harmonically varying external electric field, the time-averaged spin torque is [72]

$$\left\langle \boldsymbol{\Gamma}_{spin} \right\rangle = \frac{1}{2} |\alpha|^2 \, \mathrm{Re} \left[\frac{1}{\alpha_0^*} \mathbf{E} \times \mathbf{E}^* \right] \tag{10}$$

which causes the rotation of a particle around its own axis. In contrast, the orbit torque, which induces the rotation of particle around the optical axis, can be written as

$$\left\langle \boldsymbol{\Gamma}_{orb} \right\rangle = \mathbf{r} \times \left\langle \mathbf{F} \right\rangle, \tag{11}$$

For the traditional RP plane wave, it can be focused to generate a strong longitudinal on-axis electric field, resulting in none spin torque distribution in the equilibrium position (optical axis) for the trapped particles as depicted in Figs. 6(a) and 6(b), which show the distributions of the transverse spin torque and longitudinal orbital torque (the values are zero) in x–y plane when $z = 0.06\lambda$, respectively. Nevertheless, the trapped particles for the proposed RP CG beam always have a spin motion. This unique feature can be seen in Figs. 6(c) and 6(d). There are two lobes located symmetrically respect to the y axis for the transverse spin torque, hence trapped particles will experience spin motions around their own axes aligned in the direction parallel to the y axis. Meanwhile, the particles will rotate clockwise or anticlockwise, depending on the position where they locate. And finally, all the particles will transport to two equilibrium positions

driven by the longitudinal orbital torque, where the longitudinal orbital torque is zero.

4. Conclusions

To summarize, a new type of CG beam possessing radial polarization is proposed. With Richards and Wolf vectorial diffraction theory, all components of the electric and magnetic fields near the focus can be obtained, as well as the Poynting vectors. It is revealed that the RP CG beam exhibit totally different strong focusing properties compared with traditionally RP beams. In detail, the intensity structure of the tightly focused RP CG beam is found to exhibit strong on-axis transverse electric field, whereas the longitudinal electric field bears a shape similar to a dipole, having two lobes located symmetrically with respect to the *y* axis. The magnetic field is totally transversely polarized in the focal region, which has nearly the same pattern as that of the transverse electric field. In additional, the optical force and torque on a Rayleigh particle produced by the focused RP CG beam is also studied in detail, which indicates a stable three-dimensional trap can be achieved. Meanwhile, the trapped particles always have a spin motion. This work not only broadens the structured light field, but also delivers an important contribution towards a comprehensive understanding and application of the RP beams.

Declaration of competing interest

The authors declare that they have no known competing financial interests or personal relationships that could have appeared to influence the work reported in this paper.

Acknowledgments

References

[1] A. Ashkin, Acceleration and trapping of particles by radiation pressure, Phys. Rev. Lett. 24 (4) (1970) 156–159.

[2] A. Ashkin, Trapping of atoms by resonance radiation pressure, Phys. Rev. Lett. 40 (12) (1978) 729–732.

[3] L. Oroszi, P. Galajda, H. Kirei, S. Bottka, P. Ormos, Direct measurement of torque in an optical trap and its application to double-strand DNA, Phys. Rev. Lett. 97 (5) (2006) 058301.

[4] Q. Zhan, Trapping metallic Rayleigh particles with radial polarization, Opt. Express 12 (15) (2004) 3377–3382.

[5] M. Dienerowitz, M. Mazilu, P.J. Reece, T.F. Krauss, K. Dholakia, Optical vortex trap for resonant confinement of metal nanoparticles, Opt. Express 16 (7) (2008) 4991–4999.

[6] T.A. Nieminen, N.R. Heckenberg, H. Rubinszteindunlop, Forces in optical tweezers with radially and azimuthally polarized trapping beams, Opt. Lett. 33 (2) (2008) 122–124.

[7] Y. Zhao, D. Shapiro, D. McGloin, D.T. Chiu, S. Marchesini, Direct observation of the transfer of orbital angular momentum to metal particles from a focused circularly polarized Gaussian beam, Opt. Express 17 (25) (2009) 23316–23322.

[8] Z. Liu, D. Zhao, Radiation forces acting on a Rayleigh dielectric sphere produced by highly focused elegant Hermite-cosine-Gaussian beams, Opt. Express 20 (3) (2012) 2895–2904.

[9] L. Huang, H. Guo, J. Li, L. Ling, B. Feng, Z.Y. Li, Optical trapping of gold nanoparticles by cylindrical vector beam, Opt. Lett. 37 (10) (2012) 1694–1696.

[10] O.M. Maragò, P.H. Jones, P.G. Gucciardi, G. Volpe, A. Ferrari, Optical trapping and manipulation of nanostructures, Nat. Nanotechnol. 8 (11) (2013) 807–819.

[11] Y. Zhang, J. Wang, J. Shen, Z. Man, W. Shi, C. Min, G. Yuan, S. Zhu, H.P. Urbach, X. Yuan, Plasmonic hybridization induced trapping and manipulation of a single Au nanowire on a metallic surface, Nano Lett. 14 (2014) 6430–6436.

[12] A. Canaguier-Dur, C. Genet, Chiral route to pulling optical forces and left-handed optical torques, Phys. Rev. A 92 (2015) 043823.

[13] Y. Cao, T. Zhu, H. Lv, W. Ding, Spin-controlled orbital motion in tightly focused high-order Laguerre-Gaussian beams, Opt. Express 24 (4) (2016) 3377–3384.

[14] M. Li, S. Yan, B. Yao, Y. Liang, P. Zhang, Spinning and orbiting motion of particles in vortex beams with circular or radial polarizations, Opt. Express 24 (18) (2016) 20604–20612.

[15] A. Rahimzadegan, M. Fruhnert, R. Alaee, I. Fernandez-Corbaton, C. Rockstuhl, Optical force and torque on dipolar dual chiral particles, Phys. Rev. B 94 (2016) 125123.

[16] Z. Man, L. Du, Y. Zhang, C. Min, S. Fu, X. Yuan, Focal and optical trapping behaviors of radially polarized vortex beam with broken axial symmetry, AIP Adv. 7 (6) (2017) 065109.

[17] Y. Zhang, Y. Xue, Z. Zhu, G. Rui, Y. Cui, B. Gu, Theoretical investigation on asymmetrical spinning and orbiting motions of particles in a tightly focused power-exponent azimuthal-variant vector field, Opt. Express 26 (4) (2018) 4318–4329.

[18] G. Rui, Y. Li, S. Zhou, Y. Wang, B. Gu, Y. Cui, Q. Zhan, Optically induced rotation of Rayleigh particles by arbitrary photonic spin, Photon. Res. 7 (1) (2019) 69–79.

[19] Z. Bai, S. Zhang, Y. Lyu, R. Zhao, X. Yue, X. Ge, S. Fu, Z. Man, Metallic particle manipulation with adjustable trapping range through customized field, Opt. Commun. 473 (2020) 126045.

[20] L. Jia, E.L. Thomas, Optical forces and optical torques on various materials arising from optical lattices in the Lorentz-Mie regime, Phys. Rev. B 84 (2011) 125128.

[21] D.B. Ruffner, D.G. Grier, Optical forces and torques in nonuniform beams of light, Phys. Rev. Lett. 108 (2012) 173602.

[22] A.Y. Bekshaev, Subwavelength particles in an inhomogeneous light field: Optical forces associated with the spin and orbital energy flows, J. Opt. 15 (2013) 044004.

[23] M. Li, S. Yan, Y. Liang, P. Zhang, B. Yao, Transverse spinning of particles in highly focused vector vortex beams, Phys. Rev. A 95 (2017) 053802.

[24] A. Rahimzadegan, R. Alaee, I. Fernandez-Corbaton, C. Rockstuhl, Fundamental limits of optical force and torque, Phys. Rev. B 95 (2017) 035106.

[25] M. Li, S. Yan, Y. Liang, P. Zhang, B. Yao, Spinning of particles in optical double-vortex beams, J. Opt. 20 (2018) 025401.

[26] M. Liu, T. Zentgraf, Y. Liu, G. Bartal, X. Zhang, Light-driven nanoscale plasmonic motors, Nat. Nanotechnol. 5 (2010) 570–573.

[27] N.B. Simpson, K. Dholakia, L. Allen, M.J. Padgett, Mechanical equivalence of spin and orbital angular momentum of light: An optical spanner, Opt. Lett. 22 (1) (1997) 52–54.

[28] R. Dasgupta, S. Ahlawat, R.S. Verma, P.K. Gupta, Optical orientation and rotation of trapped red blood cells with Laguerre-Gaussian mode, Opt. Express 19 (8) (2011) 7680–7688.

[29] A.M. Yao, M.J. Padgett, Orbital angular momentum: origins, behavior and applications, Adv. Opt. Photonics 3 (2) (2011) 161–204.

[30] K.Y. Bliokh, F. Nori, Transverse and longitudinal angular momentum of light, Phys. Rep. 592 (2015) 1–38.

[31] A. Aiello, P. Banzer, M. Neugebauer, G. Leuchs, From transverse angular momentum to photonic wheels, Nat. Photonics 9 (12) (2015) 789–795.

[32] Z. Man, Z. Xi, X. Yuan, R.E. Burge, H.P. Urbach, Dual coaxial longitudinal polarization vortex structures, Phys. Rev. Lett. 124 (10) (2020) 103901.

[33] M.V. Berry, Optical currents, J. Opt. A, Pure Appl. Opt. 11 (9) (2009) 094001.

[34] A. Canaguier-Durand, A. Cuche, C. Genet, T.W. Ebbesen, Force and torque on an electric dipole by spinning light fields, Phys. Rev. A 88 (3) (2013) 033831.

[35] M. Padgett, R. Bowman, Tweezers with a twist, Nat. Photonics 5 (6) (2011) 343–348.

[36] A.T. O'Neil, I. MacVicar, L. Allen, M.J. Padgett, Intrinsic and extrinsic nature of the orbital angular momentum of a light beam, Phys. Rev. Lett. 88 (5) (2002) 053601.

[37] A. Niv, G. Biener, V. Kleiner, E. Hasman, Rotating vectorial vortices produced by space-variant subwavelength gratings, Opt. Lett. 30 (21) (2005) 2933–2935.

[38] L. Marrucci, C. Manzo, D. Paparo, Pancharatnam-Berry phase optical elements for wave front shaping in the visible domain: Switchable helical mode generation, Appl. Phys. Lett. 88 (2006) 221102.

[39] K.J. Moh, X. Yuan, J. Bu, R.E. Burge, B.Z. Gao, Generating radial or azimuthal polarization by axial sampling of circularly polarized vortex beams, Appl. Opt. 46 (30) (2007) 7544–7551.

[40] X. Wang, J. Ding, W. Ni, C. Guo, H. Wang, Generation of arbitrary vector beams with a spatial light modulator and a common path interferometric arrangement, Opt. Lett. 32 (24) (2007) 3549–3551.

[41] G.M. Lerman, U. Levy, Generation of a radially polarized light beam using space-variant subwavelength gratings at 1064 nm, Opt. Lett. 33 (23) (2008) 2782–2784.

[42] R. Zhou, B. Ibarra-Escamilla, J.W. Haus, P.E. Powers, Q. Zhan, Fiber laser generating switchable radially and azimuthally polarized beams with 140 mW output power at 1.6 um wavelength, Appl. Phys. Lett. 95 (2009) 191111.

[43] M. Bashkansky, D. Park, F.K. Fatemi, Azimuthally and radially polarized light with a nematic SLM, Opt. Express 18 (1) (2010) 212–217.

[44] X. Wang, Y. Li, J. Chen, C. Guo, J. Ding, H. Wang, A new type of vector fields with hybrid states of polarization, Opt. Express 18 (10) (2010) 10786–10795.

[45] G.M. Lerman, L. Stern, U. Levy, Generation and tight focusing of hybridly polarized vector beams, Opt. Express 18 (26) (2010) 27650–27657.

[46] H. Chen, J. Hao, B. Zhang, J. Xu, J. Ding, H. Wang, Generation of vector beam with space-variant distribution of both polarization and phase, Opt. Lett. 36 (16) (2011) 3179–3181.

[47] F. Wang, Y. Cai, Y. Dong, O. Korotkova, Experimental generation of a radially polarized beam with controllable spatial coherence, Appl. Phys. Lett. 100 (2012) 051108.

[48] S. Liu, P. Li, T. Peng, J. Zhao, Generation of arbitrary spatially variant polarization beams with a trapezoid Sagnac interferometer, Opt. Express 20 (19) (2012) 21715–21721.

[49] Z. Man, C. Min, Y. Zhang, Z. Shen, X. Yuan, Arbitrary vector beams with selective polarization states patterned by tailored polarizing films, Laser Phys. 23 (10) (2013) 105001.

[50] S. Chen, X. Zhou, Y. Liu, X. Ling, H. Luo, S. Wen, Generation of arbitrary cylindrical vector beams on the higher order Poincaré sphere, Opt. Lett. 39 (18) (2014) 5274–5276.

[51] P. Yu, S. Chen, J. Li, H. Cheng, Z. Li, W. Liu, B. Xie, Z. Liu, J. Tian, Generation of vector beams with arbitrary spatial variation of phase and linear polarization using plasmonic metasurfaces, Opt. Lett. 40 (14) (2015) 3229–3232.

[52] D. Xu, B. Gu, G. Rui, Q. Zhan, Y. Cui, Generation of arbitrary vector fields based on a pair of orthogonal elliptically polarized base vectors, Opt. Express 24 (4) (2016) 4177–4186.

[53] Z. Liu, Y. Liu, Y. Ke, Y. Liu, W. Shu, H. Luo, S. Wen, Generation of arbitrary vector vortex beams on hybrid-order Poincaré sphere, Photon. Res. 5 (1) (2017) 15–21.

[54] L. Li, C. Chang, C. Yuan, S. Feng, S. Nie, Z. Ren, H. Wang, J. Ding, High efficiency generation of tunable ellipse perfect vector beams, Photon. Res. 6 (12) (2018) 1116–1123.

[55] K.S. Youngworth, T.G. Brown, Focusing of high numerical aperture cylindrical vector beams, Opt. Express 7 (2) (2000) 77–87.

[56] Z. Man, C. Min, S. Zhu, X. Yuan, Tight focusing of quasi-cylindrically polarized beams, J. Opt. Soc. Amer. A 31 (2) (2014) 373–378.

[57] Z. Man, S. Fu, G. Wei, Focus engineering based on analytical formulae tor tightly focused polarized beams with arbitrary geometric configurations of linear polarization, J. Opt. Soc. Amer. A 34 (8) (2017) 1384–1391.

[58] Z. Man, Z. Bai, S. Zhang, J. Li, X. Li, X. Ge, Y. Zhang, S. Fu, Focusing properties of arbitrary optical fields combining spiral phase and cylindrically symmetric state of polarization, J. Opt. Soc. Amer. A 35 (6) (2018) 1014–1020.

[59] Z. Man, L. Du, C. Min, Y. Zhang, C. Zhang, S. Zhu, H.P. Urbach, X.-C. Yuan, Dynamic plasmonic beam shaping by vector beams with arbitrary locally linear polarization states, Appl. Phys. Lett. 105 (2014) 011110.

[60] B. Richards, E. Wolf, Electromagnetic diffraction in optical system II. Structure of the image field in an aplanatic system, Proc. R. Soc. Lond. Ser. A Math. Phys. Eng. Sci. 253 (1274) (1959) 358–379.

[61] Q. Zhan, Cylindrical vector beams: from mathematical concepts to applications, Adv. Opt. Photonics 1 (1) (2009) 1–57.

[62] Z. Man, X. Dou, S. Fu, Pancharatnam-Berry phase shaping for control of the transverse enhancement of focusing, Opt. Lett. 44 (2) (2019) 427–430.

[63] Z. Man, P. Meng, S. Fu, Creation of complex nano-interferometric field structures, Opt. Lett. 45 (1) (2020) 37–40.

[64] R. Dorn, S. Quabis, G. Leuchs, The focus of light—linear polarization breaks the rotational symmetry of the focal spot, J. Modern Opt. 50 (12) (2003) 1917–1926.

[65] Z. Man, Z. Bai, S. Zhang, X. Li, J. Li, X. Ge, Y. Zhang, S. Fu, Redistributing the energy flow of a tightly focused radially polarized optical field by designing phase masks, Opt. Express 26 (18) (2018) 23935–23944.

[66] W. Yuan, Z. Man, Manipulating the magnetic energy density and energy flux by cylindrically symmetric state of polarization, Optik 185 (2019) 208–214.

[67] Z. Man, X. Li, S. Zhang, Z. Bai, Y. Lyu, J. Li, X. Ge, Y. Sun, S. Fu, Manipulation of the transverse energy flow of azimuthally polarized beam in tight focusing system, Opt. Commun. 431 (2019) 174–180.

[68] Y. Lyu, Z. Man, R. Zhao, P. Meng, W. Zhang, X. Ge, S. Fu, Hybrid polarization induced transverse energy flow, Opt. Commun. 485 (2021) 126704.

[69] B.T. Draine, The discrete-dipole approximation and its application to interstellar graphite grains, Astrophys. J. 333 (1988) 848–872.

[70] C.F. Bohren, D.R. Huffman, Absorption and Scattering of Light By Small Particles, John Wiley & Sons, 2008.

[71] S. Albaladejo, M.I. Marqués, M. Laroche, J.J. Sáenz, Scattering forces from the curl of the spin angular momentum of a light field, Phys. Rev. Lett. 102 (2009) 113602.

[72] M. Li, S. Yan, B. Yao, M. Lei, Y. Yang, J. Min, D. Dan, Intrinsic optical torque of cylindrical vector beams on Rayleigh absorptive spherical particles, J. Opt. Soc. Amer. A 31 (8) (2014) 1710–1715.